

Received 15 August 2023, accepted 7 September 2023, date of publication 15 September 2023,  
date of current version 22 September 2023.

Digital Object Identifier 10.1109/ACCESS.2023.3315740

## RESEARCH ARTICLE

# A Multibeam Subarray Partition Design via Iterative Excitation Amplitude Tournament

KE WANG<sup>1</sup>, HAILIN LI<sup>1</sup>, YUAN DING<sup>2</sup>, (Member, IEEE), JING TAN<sup>1</sup>, AND XIAO DONG<sup>1</sup>

<sup>1</sup>College of Electronic and Information Engineering, Nanjing University of Aeronautics and Astronautics, Nanjing 210016, China

<sup>2</sup>School of Engineering and Physical Sciences, Heriot-Watt University, EH14 4AS Edinburgh, U.K.

Corresponding author: Hailin Li (nuaalhs@nuaa.edu.cn)

This work was supported in part by the Key Laboratory of Radar Imaging and Microwave Photonics [Nanjing University of Aeronautics and Astronautics (NUAA)], Ministry of Education under Grant NJ20220003; and in part by the Postgraduate Research and Practice Innovation Program of NUAA under Grant xcjh20220404 and Grant xcjh20220403.

**ABSTRACT** The subarray-level multibeam structure is advantageous for minimizing system complexity and enhancing multi-target detection and estimation performance. Furthermore, the subarray configuration plays a major role in determining the multibeam antenna pattern parameters. Therefore, we propose a subarray partition technique based on the tournament algorithm to enable spatial multibeam synthesis. In this paper, subarray configuration and excitation are alternately optimized through multiple rounds of tournament iterations. Each iteration calculates subarray excitations using convex optimization methods to fulfill requirements for the main radiation direction and low sidelobes, among other performance criteria. At the same time, excitations for each unassigned array element are calculated within each subarray separately. Simulation results for linear arrays demonstrate the proposed algorithm is not only suitable for linear arrays but also applicable to other array configurations, such as circular ring arrays and cylindrical arrays. And the proposed algorithm is effective in subarray periodicity, suppressing sidelobe levels, and allocating resources based on priority.

**INDEX TERMS** Antenna arrays, antenna pattern synthesis, multibeam antennas, sidelobe suppression, subarray partition.

## I. INTRODUCTION

Subarray partition technique divides the entire antenna array into several independent subarrays to achieve multi-target detection and tracking in radar and electronic countermeasure systems [1], [2]. How to segment the antenna array effectively and calculate the excitation of each segmented sparse array is a discrete, non-convex and high-order optimization problem [3].

Array segmentation strategies are roughly divided into two categories: excitation matching and heuristic methods. Excitation matching method minimizes the degree of difference between the corresponding excitation value and the predetermined excitation. Based on this thought, the tree-searching method and the border element method were proposed by optimizing the excitation amplitude, but the

excitation phase was not considered in this method [4]. Thereupon, the complex extended contiguous partition method was proposed in [5], which optimizes both amplitude and phase of the excitations. To guarantee the resulting cluster is physically contiguous, the sparsity-regularized method was used for obtaining modular clustered architectures with optimized irregular tiling configurations according to [6]. In addition, the optimal subarray partition was transformed into a clustering problem, and then a clustering method was presented to solve the array synthesis with uniform excitation at the element level in [7]. However, these methods generally require a specific reference as a prior condition. Furthermore, the excitation matching method does not allow for direct control of sidelobe levels. Heuristic methods have been successfully devised to simultaneously optimize subarray segmentation and weight. Performance indicators such as sidelobe levels or beam widths are often used as optimization goals [8]. Genetic algorithm [9], [10], differential evolution

The associate editor coordinating the review of this manuscript and approving it for publication was Hassan Tariq Chattha<sup>1</sup>.

algorithm [11], convex optimization algorithm [12], sequential convex optimization algorithm [13], and particle swarm algorithm [14] are typical examples of heuristic algorithms. Although these algorithms can achieve narrow main lobes and low sidelobes in patterns, they usually require more computing resources than the excitation matching method. In [15], the subarray design problem was formulated as a binary integer optimization problem, which was solved by iteratively relaxing the non-convex binary constraint into a convex approximation. At this time, the heuristic initial iteration point was set randomly according to [15]. To find solutions that provide exact tilting and scanning radiation performance simultaneously, the heuristic iterative convex relaxation programming (H-ICRP) framework [16] was proposed, which finds a heuristic initial point. In [17], the initial point was first set using the excitation matching strategy, and then the subarray design scheme was obtained by an iterative convex optimization algorithm with the weighted L1 norm. By combining the advantages of the excitation matching method and heuristic algorithm, this method improves search performance and avoids falling into local convergence.

Due to the anisotropy of array elements, a general partition method for arbitrary phased array structures has not yet been reported. Most algorithms are only suitable for specific arrays. There are many methods that perform well for subarray partition and beam pattern in linear arrays. For example, an efficient method based on compressed sensing (CS) was proposed in [18]. Additionally, improved particle swarm algorithms [14] and hybrid algorithms of genetic and convex optimization [19] have been proposed to obtain optimal configurations using heuristic methods. To synthesize asymmetric shaped beam patterns, a novel clustering method combining linear programming and nested K-means methods was proposed in [20]. The rectangular array is also a common antenna array structure. An improved genetic algorithm was used to complete the array element allocation and suppress sidelobe levels as demonstrated in [21]. In order to break the periodic array layout and simplify the feeding network, a type of single-shaped subarray was proposed by flipping and filling the aperture. Consequently, a type of single-shaped subarray with different orientations was proposed in [22], and the L-shaped subarray was proposed in [23] to suppress sidelobe levels and reduce complexity, which is beneficial for both manufacturing and maintenance. However, with changes in the array structure, the design structure of the subarray will subsequently change. More subarray partition methods have been applied to arrays of other structures to meet practical engineering needs. For example, the K-means clustering method proposed in [3] and [24] can be used to design subarrays for linear and rectangular arrays. Additionally, an efficient iterative algorithm using penalty-based optimization methods was proposed in [25] to solve uniformly and non-uniformly spaced subarray configurations. It optimizes subarray configurations and element excitations/positions with minimum inter-element spacing simultaneously to minimize peak sidelobe levels. Subarray partition methods are

currently being adopted in some special conformal array antennas. In [26], precise partition methods and quasi-precise partition methods of the X algorithm were used in the circular array. Sivasankar and Hegde used a weighted clustering algorithm to obtain subarray configurations and multibeam patterns in the hexagonal array in [27]. The differential evolution algorithm proposed in [28] is beneficial for finding subarray configurations for arc arrays. And in [29] proposed a design for concentric ring antenna arrays to simplify the feeding system.

This paper proposes a subarray partition method for array antennas using an excitation amplitude tournament. Compared with other algorithms, the proposed algorithm divides the array into subarrays by selecting apertures. The main contributions of this article can be summarized as follows: 1) Instead of relying solely on an excitation matching or heuristic method, our proposed algorithm combines the basic knowledge of array aperture and convex optimization algorithms to solve the discrete and non-convex problem. 2) The proposed algorithm addresses the issue of non-uniform and discontinuous partitioning of three-dimensional conformal array antennas. 3) Compared to other algorithms for the subarray partition of line arrays, the subarray configuration can be obtained with lower sidelobe levels.

The remainder of the paper is organized as follows. Section II describes the mathematical formulation of the multibeam pattern synthesis based on the proposed subarray partition technique, and how the exact partition of the antenna array aperture is converted into an optimized problem concerning subarray partition and excitation. In order to solve the complex non-convex optimization problem, Section III uses an amplitude tournament competition of the excitations to ensure the subarray configuration. The beam pattern synthesis with low sidelobe performance is then obtained by optimizing the subarray partition scheme and excitation weight. In Section IV, some representative results from a set of numerical experiments are presented and discussed. Finally, Section V summarizes the conclusions and prospects of this research.

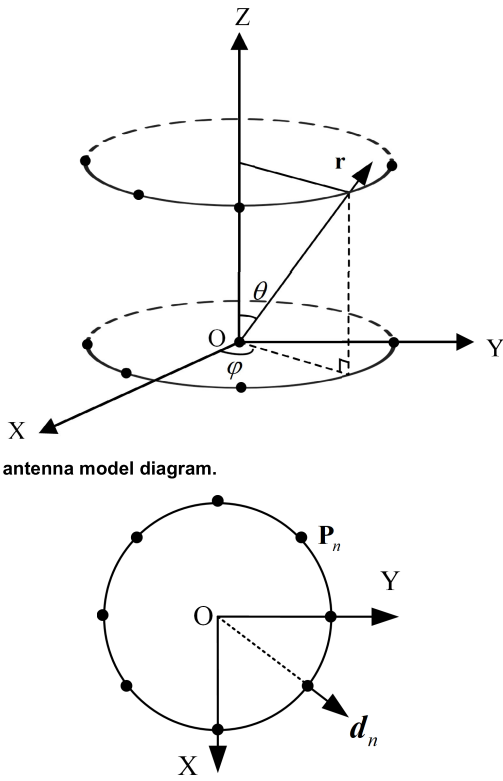
## II. MATHEMATIC MODEL

Our proposed algorithm is not only applicable to linear arrays but also suitable for other conformal arrays. Then, we construct a mathematical model using a cylindrical array as an example. Fig. 1 shows the schematic diagram of the array antenna, where each small radiating dot represents an antenna element.

The far-field radiation intensity of an array antenna is

$$E(\mathbf{r}) = \sum_{n=1}^N w_n f(\Delta_n) \exp(jK \mathbf{P}_n^T \mathbf{r}), \quad (1)$$

where  $N$  is the number of array elements.  $w_n$ ,  $\mathbf{P}_n = [x_n \ y_n \ z_n]^T$  and  $f(\Delta_n)$  are the excitation coefficient, position vector and electric field intensity of the  $n^{\text{th}}$  element, respectively. Define  $K = 2\pi f_0/c$ , where  $c$  is the light velocity, and  $f_0$  is the center frequency.



(a) Array antenna model diagram.

(b) Element arrangement diagram.

FIGURE 1. Schematic diagram of array antenna.

The  $\mathbf{r} = [\sin\theta\cos\varphi \ \sin\theta\sin\varphi \ \cos\theta]^T$  is a unit vector, where  $\theta$  and  $\varphi$  are noted as the elevation angle and azimuth angle, respectively. In addition,  $\Delta_n = \arccos(\mathbf{d}_n^T \mathbf{r})$  is the angle in-between the normal vector direction  $\mathbf{d}_n$  and the radiation direction  $\mathbf{r}$  of the  $n^{\text{th}}$  element. Therefore, we can know that the normal vectors  $\mathbf{d}_n$  of the  $n^{\text{th}}$  element points outward from the center of the circular ring.

Referring to (1), the far-field radiation intensity can be written as

$$E(\mathbf{r}) = \mathbf{w}^T \mathbf{b}, \quad (2)$$

where  $\mathbf{w} = [w_1 \ w_2 \ \dots \ w_N]^T$  is the complex excitation vector and the array steering vector is expressed as  $\mathbf{b} = [f(\Delta_1)\exp(jK\mathbf{P}_1^T \mathbf{r}) \ \dots \ f(\Delta_N)\exp(jK\mathbf{P}_N^T \mathbf{r})]^T$ .

To synthesize a multibeam pattern, we can optimize the amplitude and phase of excitation. In order to generate beams in multiple desired directions, we need to meet the following requirements:

- 1) Minimize the sidelobe levels (SLLs).
- 2) Meet a given value of the radiation level in the targeted beamforming direction.

Thus, the optimization model can be summarized as follows:

$$\begin{aligned} \min_w \quad & \varepsilon \\ \text{s.t.} \quad & \mathbf{w}^T \mathbf{b}_r = \mu, \\ & |\mathbf{w}^T \mathbf{b}_s| \leq \varepsilon, \mathbf{r}_s \in \Omega_s \\ & |\mathbf{w}| \leq 1 \end{aligned} \quad (3)$$

where  $\mathbf{w}^T \mathbf{b}_r$  and  $\mathbf{w}^T \mathbf{b}_s$  are respectively noted as the radiation intensity in the radiation direction  $\mathbf{r}$  and in the sampling direction  $\mathbf{r}_s$ .  $\mu$  is the given expected radiation value, and  $\varepsilon$  denotes the sidelobe constraint parameter in the sidelobe region  $\Omega_s$ . Excitation amplitude  $|\mathbf{w}|$  is normalized.

Subarray partition technique divides the array into different independent apertures. Then, the radiation field intensity of the  $m^{\text{th}}$  subarray is defined as

$$E_m(\mathbf{r}) = \sum_{n=1}^N \beta_{nm} w_n f(\Delta_{nm}) \exp(jK\mathbf{P}_n^T \mathbf{r}), \quad (4)$$

where  $\beta_{nm}$  represents the working state about the  $n^{\text{th}}$  element in the  $m^{\text{th}}$  subarray. The binary variable  $\beta_{nm}$  describes the working state and it satisfies  $\forall n, \sum_{m=1}^M \beta_{nm} \leq 1$ . Where  $\beta_{nm} = 1$  means that the  $n^{\text{th}}$  element is working at the  $m^{\text{th}}$  subarray, and  $\beta_{nm} = 0$  means that it is not.

From (3) and (5), we can conclude the radiation intensity based on subarray partition technique as

$$E(\mathbf{r}) = \sum_{m=1}^M \sum_{n=1}^N \beta_{nm} w_n f(\Delta_{nm}) \exp(jK\mathbf{P}_n^T \mathbf{r}). \quad (5)$$

To satisfy the requirements of array pattern synthesis, multibeam pattern synthesis based on subarray partition needs to meet the following conditions:

- 1) Each element is not shared by multiple subarrays.
- 2) Each radiation level along beamforming direction is greater than the given value.
- 3) Each subarray generates a beam  $s$  that satisfies the sidelobe constraint.

Therefore, the comprehensive mathematical model of multibeam pattern can be expressed as in (6).

$$\begin{aligned} \max_{\beta_m, \mathbf{w}} \quad & \mu_m \\ \text{s.t.} \quad & (\beta_m \mathbf{w})^T \mathbf{b}_m = \mu_m \\ & |(\beta_m \mathbf{w})^T \mathbf{b}_{ms}| \leq \varepsilon_m, \mathbf{r}_{ms} \in \Omega_{ms}. \\ & 0 \leq \sum_m \beta_m \leq 1 \\ & \beta_{nm} \in \{0, 1\} \end{aligned} \quad (6)$$

Suppose the division configuration of the  $m^{\text{th}}$  subarray is  $\beta_m = [\beta_{1m} \ \dots \ \beta_{Nm}]^T$ .  $\mathbf{b}_{ms}$  is the array steering vector in the area of the sideband. At the same time,  $\mu_m$  and  $\varepsilon_m$  are the expected amplitude and sidelobe constraint, respectively.

The mathematical model becomes an optimization problem with multiple variables, where  $\beta_{nm}$  is a binary variable. So, we cannot solve the problem directly by the convex optimization algorithm.

### III. METHOD OF TOURNAMENT COMPETITION

Because the problem (6) cannot be solved by the current solvers, this paper proposes a method based on the excitation amplitude tournament competition to find the selecting vector  $\beta_m$ . After that, the mathematical model is transformed into

a convex optimization problem to get the multibeam pattern synthesis with desired sidelobe levels.

The algorithm is carried out from the following three aspects.

**A. MAXIMIZE SUBARRAY APERTURE**

The aperture size of the array antenna negatively affects the sidelobe performance. As the number of elements decreases and the aperture size decreases, the sidelobe level increases. So, in order to obtain a low sidelobe level, it is desirable for each subarray to obtain the maximum aperture size. Therefore, the initial array elements of each subarray can be determined by maximizing the aperture.

The array antenna of  $N$  elements is divided into  $M$  subarrays, so the  $m^{th}$  subarray contains  $N_m$  elements meeting  $\sum_{m=1}^M N_m \leq N$ . We use the position vector  $\mathbf{P}_n$  to describe the  $n^{th}$  element. Defining the  $m^{th}$  subarray set  $A_m$  that is composed of the selectable element position  $\mathbf{P}_n$ , we can write it as

$$A_m = \{\mathbf{P}_n, \forall n, f(\Delta_{nm}) > 0\}, \quad (7)$$

where  $\Delta_{nm}$  represents the angle between the normal vector  $\mathbf{d}_n$  and the radiation direction  $\mathbf{r}_m$  of the  $m^{th}$  subarray.

The maximum aperture of the  $m^{th}$  subarray is determined by

$$R_m = \max(\|\mathbf{P}_i - \mathbf{P}_j\|_2), \quad \forall \mathbf{P}_i, \mathbf{P}_j \in A_m. \quad (8)$$

Referring to (4), suppose  $\mathbf{P}_{k1}, \mathbf{P}_{k2}$  are the largest two aperture positions for the  $m^{th}$  subarray. So, the subarray partition coefficient  $\beta_{nm}$  meets

$$\beta_{nm} = \begin{cases} 1 & m \\ 0 & else, \end{cases} \quad n \in \{k_1, k_2\}. \quad (9)$$

The initial subarray selection set is  $S_m^0 = \{\mathbf{P}_{m1}, \mathbf{P}_{m2}\}$ , and  $\mathbf{P}_{m1}, \mathbf{P}_{m2}$  generally are expressed by the largest two aperture positions. If the aperture position is occupied by other subarrays, we can select the second-largest apertures referring to (8). Then the  $m^{th}$  subarray selection set is  $S_m$ .

Correspondingly, the remaining  $N - 2M$  elements are divided into the initial candidate sequence  $S_0^0 = \{\mathbf{P}_n, \forall n, m, \mathbf{P}_n \notin S_m, \mathbf{P}_n \in A_m\}$ .

**B. OPTIMIZE EXCITATION VALUE**

Once the subarray selecting vector  $\beta_m$  is determined, the problem (6) is transformed into a single-beam synthesis problem.

When the main lobe gain  $E_m(\mathbf{r}) = 1$ , we can get the optimal excitation value. Then the mathematical model becomes

$$\begin{aligned} \min_w \quad & \varepsilon_m \\ \text{s.t.} \quad & \mathbf{w}^T \mathbf{b}_m = 1. \\ & |\mathbf{w}^T \mathbf{b}_{ms}| \leq \varepsilon_m, r_{ms} \in \Omega_{ms} \\ & |\mathbf{w}| \leq 1 \end{aligned} \quad (10)$$

The complex excitation coefficient is generally expressed as

$$w_n = I_n e^{j\psi_n}, \quad (11)$$

where  $I_n \in [0, 1]$  and  $\psi_n$  are the excitation amplitude and phase of the  $n^{th}$  array element, respectively.

Referring to (10), we can obtain the weight  $\mathbf{w}$  by the convex optimization algorithm (CVX). It is used to evaluate the contribution of each element in multiple given directions. The maximum gain is  $\mu_m = 1/\max(\mathbf{w})$ .

**C. MAXIMIZE SUBARRAY RADIATION LEVEL**

According to (4), the maximum radiation intensity in the radiation direction  $\mathbf{r}_m$  is

$$|E_m(\mathbf{r}_m)|_{\max} = \sum_{n=1}^N \beta_{nm} f(\Delta_{nm}), \quad \forall n, \mathbf{P}_n \in A_m, \quad (12)$$

where the excitation amplitude and phase are  $I_n = 1$  and  $\psi_n = -jK \mathbf{P}_n^T \mathbf{r}$ , respectively. The radiation power is negatively correlated to the sidelobe performance. To meet the low sidelobe levels, the maximum radiation intensity  $|E_m(\mathbf{r}_m)|_{\max}$  should be larger than the given value  $\mu_m$ . Let  $|E_m(\mathbf{r}_m)| = \beta_m^T \mathbf{F}_m$ , can be expressed as

$$\begin{aligned} \max \quad & \mu_0 \\ \text{s.t.} \quad & \mu_m + \mu_0 = \beta_m^T \mathbf{F}_m, \end{aligned} \quad (13)$$

where  $\mu_m$  is the given radiation value and  $\mu_0$  is the gain redundancy.  $\mathbf{F}_m = [f(\Delta_{1m}) \dots f(\Delta_{Nm})]$  represents the radiation intensity, and  $\beta_m = [\beta_{1m} \dots \beta_{Nm}]^T$  is the partition result of the  $m^{th}$  subarray in the radiation direction  $\mathbf{r}_m$ .

To obtain high radiation gain, the selection sequence  $S_m^i$  should be composed of array elements with the large radiation intensity value  $f(\Delta_{nm})$  from the candidate array element set  $S_0^i$ . Suppose that the element position with the highest radiation intensity is  $\mathbf{P}_{\max}$ . If  $|E_m^{i+1}(\mathbf{r})|_{\max} < \mu_m + \mu_0$ , we should update the selection set and candidate sequence of  $i + 1$  times is  $S_m^{i+1} = \{S_m^i, \mathbf{P}_{\max}\}, S_0^{i+1} = S_0^i - \{\mathbf{P}_{\max}\}$ . Otherwise, we should keep  $S_m^{i+1}, S_0^{i+1}$  and  $S_m^i, S_0^i$  consistent.

In each round of the tournament, according to (11) and (13), we can obtain that the excitation amplitude and the radiation intensity of the  $m^{th}$  subarray are  $I_{nm}^{i+1}, \forall n, \mathbf{P}_n \in S_0^i$  and  $I_{nm}^{i+1} f(\Delta_{nm}), \forall n, \mathbf{P}_n \in S_0^i$ .

In this section, we propose an array element partition method based on the competition of excitation amplitude tournament. The method involves the following steps:

- 1) Maximize the subarray aperture to determine the initial subarray.
- 2) Minimize the sidelobe level to optimize the complex excitation coefficients.
- 3) Maximize the subarray radiation gain to update subarray sequence and obtain the multibeam pattern.

The flowchart is shown in Fig. 2, and the processing flow is given below.

Step 1) Initialize the array parameters and multibeam values. Input parameters such as the number of array elements,

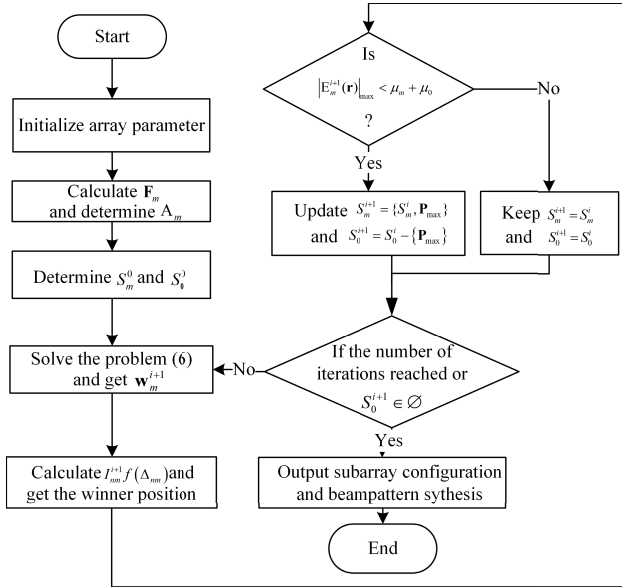


FIGURE 2. Flowchart of proposed algorithm.

the number of winning-element, and the expected amplitude for calculation.

Step 2) Solve the element radiation intensity vector  $f(\Delta_{nm})$  and construct the candidate array element sequence  $A_m$ .

Step 3) Determine the initial element selection set of each subarray  $S_m^0$  and the candidate set  $S_0^0$ .

Step 4) If the set  $S_0^{i+1}$  is not empty or the tournament iterations do not reach the maximum number, we should repeat the following steps:

1) According to the single beam pattern synthesis in (10), solve the excitation coefficient  $w_m^{i+1}$  and excitation amplitude  $I_{nm}^{i+1}$ .

2) Select the element with the largest radiation intensity  $I_{nm}^{i+1} f(\Delta_{nm})$  as the winner  $P_m$  of the tournament competition.

3) Update the array element selection sequence  $S_m^{i+1}$  and the candidate set  $S_0^{i+1}$ .

Step 5) The entire array segmentation is completed based on the task priorities. Output subarray configuration and multibeam pattern synthesis.

#### IV. SIMULATION RESULTS

In this section, we present a series of numerical examples to assess the feasibility and validity of the proposed method. In order to comprehensively analyze the algorithm and its performance, we also explore the effects of various parameters on the algorithm's performance. All simulations were calculated in MATLAB R2018a, and the computer configuration was an i5 10500 CPU with 8GB of memory.

##### A. LINEAR ARRAY MULTIBEAM PATTERN SYNTHESIS BASED ON SUBARRAY PARTITION

In this section, we compare the beam pattern performance of the proposed method with the block partition method (BPM) to verify the superiority in terms of main lobe width

and maximum sidelobe level suppression performance. Suppose a uniform linear array with 40-element spaced by half-wavelength is considered. The beam width is  $10^\circ$ , and the respected radiations are set as  $\theta_1 = -30^\circ$ ,  $\theta_2 = 0^\circ$ ,  $\theta_3 = 30^\circ$ . Table 1 lists the comparison of simulation results.

TABLE 1. Comparison of simulation results for two algorithms.

	Proposed Method			BPM		
$\theta$ ( $^\circ$ )	-30	0	30	-30	0	30
SLL (dB)	-11.26	-10.49	-11.18	-10.09	-7.52	-9.03
Elements	15	11	14	15	11	14

Fig. 3 shows the subarray partition results in detail. Meanwhile, Fig. 4 shows the multibeam pattern synthesis using subarray partition.

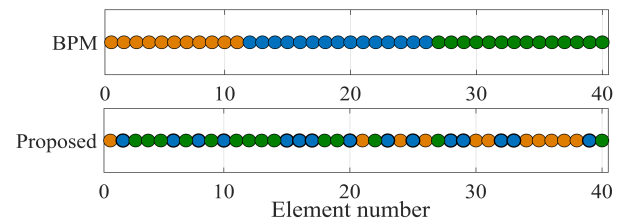


FIGURE 3. Subarray configuration of the proposed method and block partition method. The yellow, blue, and green marks indicate that the element belongs to the subarray at  $\theta_1 = -30^\circ$ ,  $\theta_2 = 0^\circ$  and  $\theta_3 = 30^\circ$ , respectively.

As problem (6) is non-convex, the proposed method solves the problem. In this section, we compare our algorithm and a hybrid algorithm in [19] to verify the effectiveness.

For intuitive display, a linear array composed of 40 isotropic elements is considered. The desired radiation directions are  $\{-5^\circ, 15^\circ\}$  and the corresponding sidelobe region is  $[-90^\circ, -10^\circ] \cup [0^\circ, 10^\circ] \cup [20^\circ, 90^\circ]$ . Table 2 lists the sidelobe levels of the proposed method and the hybrid algorithm.

From that, we can conclude that: 1) the proposed method effectively solves the non-convex problem. 2) the peak sidelobe level of the proposed method is lower than that of the hybrid algorithm.

##### B. PERFORMANCE ANALYSIS OF DIFFERENT PARAMETERS

In this experiment, we aim at showing the capability of the proposed method to discuss the performance with different parameters. We also select the uniform linear array as an example.

##### 1) THE COMPARISON WITH DIFFERENT WINNING-ELEMENTS

The proposed algorithm divides the array based on the predetermined number of winning-element for each iteration.



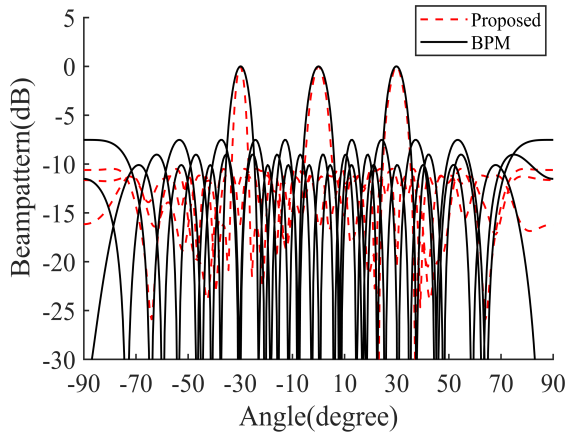


FIGURE 4. Two-dimensional pattern by the proposed method and BPM. The red and black type line denote the subarray pattern synthesis with the proposed method and BPM.

TABLE 2. Sidelobe levels by the proposed method and the method in [19].

Method	Proposed Algorithm		Method in [19]	
$\theta$ (°)	-5	15	-5	15
SLL (dB)	-18.17	-18.45	-17.12	-17.12

In this part, we mainly focus on the effect of the different number of winning-element on running time and sidelobe level.

The uniform linear array consists of 100-element spaced by half-wavelength and the beam width is 10°. Assuming that the three respected radiations are sequentially set as  $\theta_1 = -30^\circ, \theta_2 = 0^\circ, \theta_3 = 30^\circ$ . Under limited resources, the priority order of the three tasks also follows this order. Table 3 reflects the variation law of the running time.

TABLE 3. The variation law of the running time with different values.

Winning-element ( $N_w$ )	1	2	3	4	5
Iteration Times	40	25	20	16	10
Operation Time (s)	94.58	55.98	50.92	36.38	35.20

It can be seen from Table 3 that with the increase of  $N_w$ , the iteration times and operation time are decreasing. Then the side-lobe levels are summarized in Fig. 5 in detail. We can see that the SLLs of the subarray multibeam pattern are controlled below -19.55 dB, -18.36 dB, -16.44 dB, -15.83 dB, and -15.63 dB, respectively.

There is a tradeoff between the sidelobe levels and the operation time. We can conclude that: 1) with  $N_w$  increasing, the iteration times and operation time decrease. 2) with increasing, the sidelobe levels of each subarray increases.

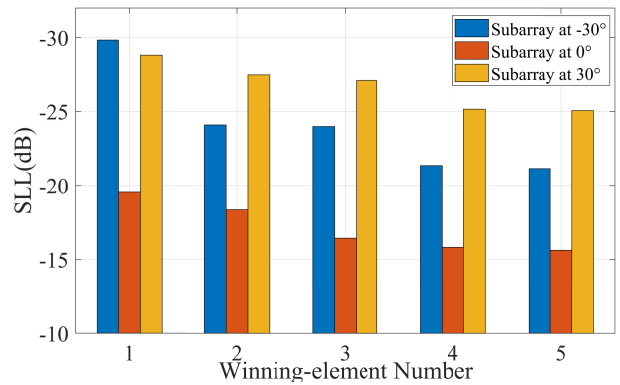


FIGURE 5. Variation law of the sidelobe level for each subarray.

### 2) THE COMPARISON WITH DIFFERENT PRIORITY ORDER

In this section, the proposed algorithm can allocate array according to the radiation demand, and assign the elements with high radiant intensity to the subarray based on priority order.

A uniform linear array of 40 elements is selected. And we also set a series of experiments to explore the effect of the priority order on the performance. Table 4 shows the performance in different configurations and sidelobe levels with two different orders. The order 1 is set to  $-30^\circ, 0^\circ, 30^\circ$ , and the order 2 is set to  $30^\circ, 0^\circ, -30^\circ$ .

TABLE 4. Performance parameters for different priority orders.

Parameter	Sequence 1			Sequence 2		
$\theta$ (°)	-30	0	30	-30	0	30
SLL (dB)	-12.54	-8.72	-10.55	-10.55	-8.72	-12.54
Elements	14	13	13	13	13	14

Meanwhile, the number of iterations is set to 12, and the iteration time is 14.41 seconds and 14.44 seconds, respectively.

Based on these results, we can draw the following conclusions: 1) changing the priority order leads to a reduction in subarray elements and an increase in sidelobe levels. 2) changing the priority order has little effect on iteration times and computation time.

### 3) THE COMPARISON WITH DIFFERENT ELEMENT NUMBER

As we all know, the number of array elements can affect the performance of the multibeam pattern. Therefore, we explore the algorithm performance with different the number of elements for the array antenna.

We select a uniform linear array with varying numbers of elements  $N$ . The variation of running time is listed in Table 5, while the variation of subarray configuration and sidelobe levels are listed in Table 6. Since the variation trend of the sidelobe levels for each subarray is analogous, Fig. 6 only

**TABLE 5. Variation law of the running time.**

Elements (N)	30	40	50	60	70
Iteration times	16	22	28	34	41
Operation time (s)	20.83	32.39	42.20	63.17	82.16

**TABLE 6. Variation law of performance parameters for the proposed method.**

Elements	Elements Quantity			SLL (dB)		
	-30°	0°	30°	-30°	0°	30°
N=30	11	9	10	-9.63	-7.31	-8.70
N=40	15	11	14	-12.54	-8.72	-10.55
N=50	18	14	18	-13.67	-12.21	-14.02
N=60	22	16	22	-16.78	-12.82	-18.27
N=70	26	19	25	-19.86	-12.98	-18.45

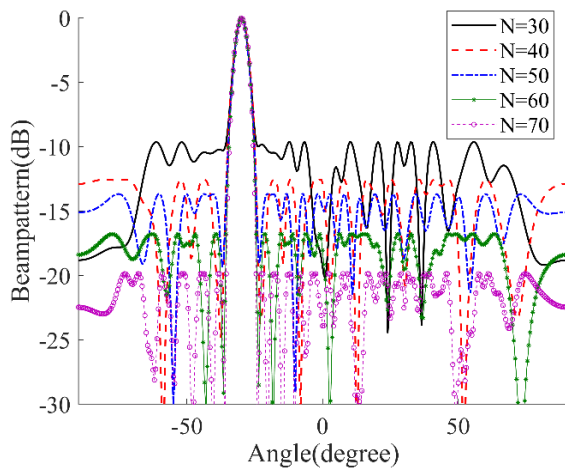


**FIGURE 6. The beam pattern of the sidelobe level in the radiation direction with different total element number.**

shows the beam pattern in radiation direction  $\theta_1 = -30^\circ$  with different array element numbers.

As the number of elements decreases from 70 to 30, the operation time of the algorithm is reduced by 61.33 seconds. Additionally, the sidelobe levels of the three beams increase by 10.53 dB, 5.67 dB, and 9.75 dB, respectively.

#### 4) THE COMPARISON WITH DIFFERENT EXPECTED MAGNITUDE

Due to the proposed algorithm allocating array elements while meeting radiation requirements. Therefore, we explore the impact of different radiation requirements on algorithm performance.

In this part, the uniform linear array consists of 40-element with the space setting to  $\lambda/2$  and the beam width setting to  $10^\circ$ . We explore the effect by keeping the expected

amplitude  $\mu_2 = \mu_3 = 3$  unchanged, and altering the expected amplitude  $\mu_1$ .

Therefore, the values  $\mu_1$  are set as Table 7. And Table 7 shows the results in sidelobe levels and subarray configurations with different values. For the sake of clarity, Fig. 7 summarizes the variation law of the sidelobe level of each subarray in detail.

**TABLE 7. Variation law of performance parameters for the proposed method.**

$\mu_1$	Elements Quantity			SLL (dB)		
	-30°	0°	30°	-30°	0°	30°
1	13	12	15	-9.31	-9.14	-12.01
3	15	11	14	-12.54	-8.72	-10.55
5	17	10	13	-14.11	-7.26	-10.78
7	18	10	12	-12.95	-6.70	-8.26
9	20	9	11	-15.91	-6.33	-8.02

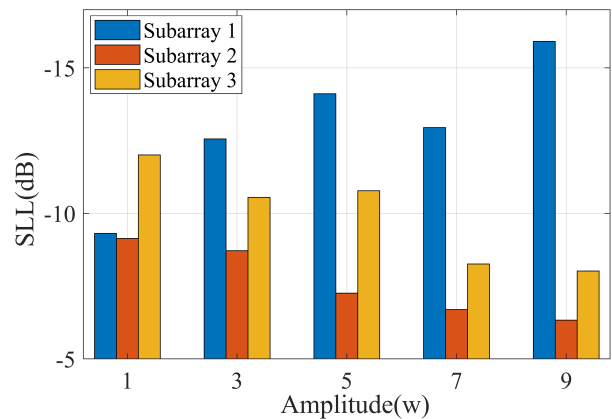


**FIGURE 7. Variation law of the sidelobe level for each subarray.**

As the expected amplitude increases from 1 to 9, the sidelobe level of the first beam decreases by 6.6 dB, and the corresponding number of subarray elements increases by 7. However, for subarrays 2 and 3, the sidelobe levels increase by 2.81 dB and 3.99 dB, respectively. The element numbers of these subarrays also decrease by 3 and 4.

The above simulation results indicate that the partition results remain unchanged under the same given conditions. Meanwhile, the local optimum of the convex optimization algorithm is the global optimum. The tournament strategy is advantageous in finding the global optimum. So, convergence analysis shows the effectiveness of the proposed algorithm.

#### C. CIRCULAR AND CYLINDRICAL MULTIBEAM PATTERN SYNTHESIS BASED ON SUBARRAY DIVISION

Due to the anisotropy of the radiation pattern, the structure of most conformal arrays is more complex than that of linear arrays. In order to further explore whether the proposed

algorithm is suitable for array antennas, this section selects circular arrays and cylindrical arrays as simulation examples.

1) SUBARRAY PARTITION AND PATTERN SYNTHESIS OF CIRCULAR ARRAY ANTENNA

In this section, a 300-element three-dimensional torus with the beam width of  $10^\circ$  is selected for simulation. The elevation angles are set to  $\theta_1 = \theta_2 = \theta_3 = 90^\circ$  and azimuth angles are set to  $\varphi_1 = 90^\circ, \varphi_2 = 100^\circ, \varphi_3 = 110^\circ$ . The radius is set to  $5\lambda$ . And each array element is located on the torus spaced at equal angles. Table 8 shows the performance of the pattern on subarray configuration and sidelobe level.

TABLE 8. Performance of subarray partition.

Parameter	Subarray 1	Subarray 2	Subarray 3
$\theta$ ( $^\circ$ )	90	90	90
$\varphi$ ( $^\circ$ )	90	100	110
SLL (dB)	-20.50	-21.00	-22.88
Elements	53	57	56

Fig. 8 shows the synthesis of subarray multibeam patterns for the circular array antenna, and the subarray configuration obtained by the proposed method is listed in Fig. 9.

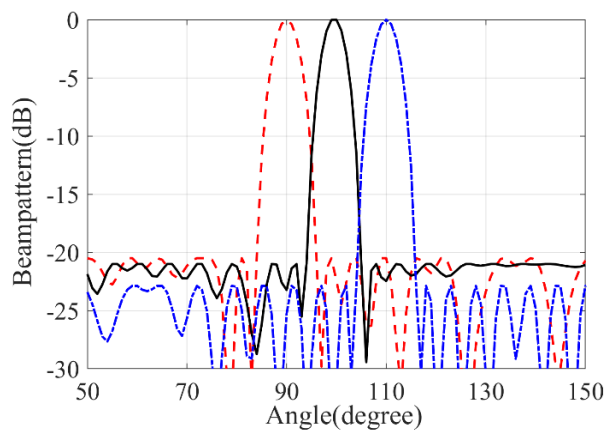


FIGURE 8. The subarray multibeam pattern synthesis by the proposed algorithm. The line with red, black, and blue indicate the subarray at  $\theta_0 = 90^\circ, \varphi_0 = 90^\circ, \theta_1 = 90^\circ, \varphi_1 = 110^\circ$ , and  $\theta_2 = 90^\circ, \varphi_2 = 90^\circ$ , respectively.

Fig. 9 only shows 166 elements out of the 320 elements, which have been calculated to be in working condition. Due to the complex structure and large number of elements in large-scale array antennas, effective array elements are preselected to form subarrays according to the relationship between the array structure and radiation direction. These effective array elements are defined as working array elements, which help improve calculation speed.

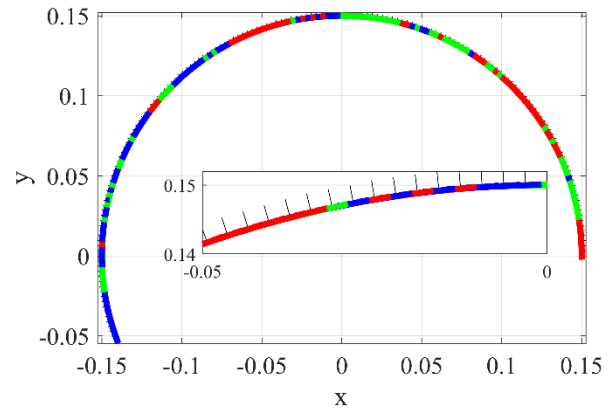


FIGURE 9. The subarray configuration obtained by the proposed algorithm. Red, green, and blue mark indicate that the element belongs to the subarray at  $\theta_0 = 90^\circ, \varphi_0 = 90^\circ, \theta_1 = 90^\circ, \varphi_1 = 110^\circ$ , and  $\theta_2 = 90^\circ, \varphi_2 = 90^\circ$ , respectively.

The circular array has lower sparsity and dispersion compared to the linear array due to non-uniform positions and orientations. Pencil subarray beams with equal amplitude are synthesized by the proposed algorithm in three radiation directions, and the average sidelobe level is controlled below  $-20$  dB.

From these results, we can see that the proposed method is valid for subarray partition and multibeam pattern synthesis with low sidelobe level in circular array antennas.

2) SUBARRAY PARTITION AND PATTERN SYNTHESIS OF CYLINDRICAL ARRAY ANTENNA

This section selects a three-dimensional cylinder with 320 array elements for simulation. Suppose that the two desired beam directions are  $\theta_0 = 90^\circ, \varphi_0 = 50^\circ$  and  $\theta_1 = 90^\circ, \varphi_1 = 70^\circ$ . The performance of the three-dimensional cylindrical array elements are shown in Table 9.

TABLE 9. Performance of cylindrical subarray partition.

Parameter	Subarray 1	Subarray 2
$\theta_0, \theta_1$ ( $^\circ$ )	90	90
$\varphi_0, \varphi_1$ ( $^\circ$ )	50	70
SLL (dB)	-18.75	-16.03
Elements	60	60

Fig. 10 shows the detailed subarray layout for the elements in working state, and the three-dimensional beam patterns of the two beams are shown in Fig. 11.

From Fig. 10, we can see that there are 120 elements in the working state, and the proposed algorithm efficiently completes the partition of overlapping regions. The core of the



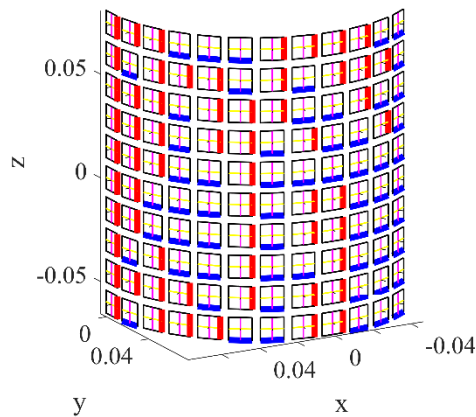


**FIGURE 10.** 3D cylindrical subarray configuration. Red and blue are used to indicate that the element belongs to the  $\theta_0 = 90^\circ$ ,  $\varphi_0 = 50^\circ$  and  $\theta_1 = 90^\circ$ ,  $\varphi_1 = 70^\circ$ , respectively.

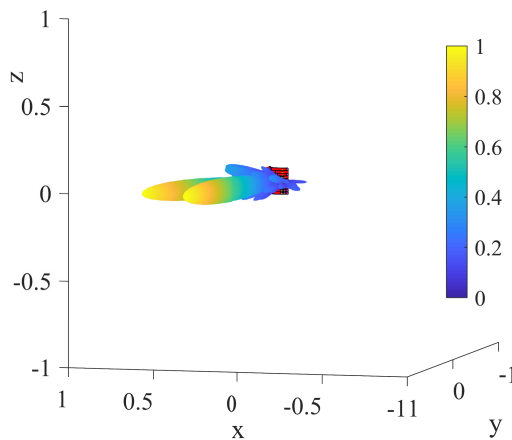


**FIGURE 11.** Three-dimensional beam pattern of multibeam simultaneously. One beam is at  $\theta_0 = 90^\circ$ ,  $\varphi_0 = 50^\circ$  and the other is at  $\theta_1 = 90^\circ$ ,  $\varphi_1 = 70^\circ$ .

design is dividing the elements into corresponding subarrays according to the radiation intensity. After dividing the array, each of the two subarrays has 60 elements. At the same time, the sidelobe level of each beam is controlled below an average of  $-16$  dB.

From these results, we can see that the proposed method is suitable for both 3D circular arrays and 3D cylindrical arrays. Therefore, the algorithm is feasible and effective for cylindrical array configurations. It also performs well in suppressing the sidelobe level.

## V. CONCLUSION

This paper presents a new method based on excitation amplitude competition. By utilizing the relationship between the aperture and sidelobe level, the proposed method obtains a subarray partition scheme and multibeam pattern synthesis by optimizing the subarray configuration and excitation.

The main contributions of this article can be summarized as follows: 1) The proposed algorithm is not only suitable

for linear arrays but also applicable to other array configurations. 2) Solving the discrete and non-convex problem of the subarray configuration scheme through combining the basic knowledge of array aperture and optimization algorithms. 3) Synthesizing subarray multibeam patterns with low sidelobe levels that meet multi-function needs by properly dividing antenna resources based on the priority order of multiple tasks.

Future work will involve exploring the effect of device errors on subarray configuration and beam pattern design.

## REFERENCES

- [1] C. Wei, X. Yu, Y. Chen, and Z. Hu, "A multi-task subarray selection approach for large linear antenna arrays," *IEEE Access*, vol. 8, pp. 17438–17448, 2020.
- [2] F. Liu, J. Li, D. Liu, and X. Li, "Low-complexity subarray grouping algorithm for millimeter-wave massive MIMO systems," *IEEE Access*, vol. 7, pp. 14300–14312, 2019.
- [3] Q. H. Shi, Z. Zheng, and Y. Sun, "Pattern synthesis of subarrayed large linear and planar arrays using K-means solution," *IEEE Antennas Wireless Propag. Lett.*, vol. 20, no. 5, pp. 693–697, May 2021.
- [4] L. Manica, P. Rocca, A. Martini, and A. Massa, "An innovative approach based on a tree-searching algorithm for the optimal matching of independently optimum sum and difference excitations," *IEEE Trans. Antennas Propag.*, vol. 56, no. 1, pp. 58–66, Jan. 2008.
- [5] P. Rocca, L. Poli, A. Polo, and A. Massa, "Optimal excitation matching strategy for sub-arrayed phased linear arrays generating arbitrary-shaped beams," *IEEE Trans. Antennas Propag.*, vol. 68, no. 6, pp. 4638–4647, Jun. 2020.
- [6] G. Oliveri, M. Salucci, and A. Massa, "Synthesis of modular contiguously clustered linear arrays through a sparseness-regularized solver," *IEEE Trans. Antennas Propag.*, vol. 64, no. 10, pp. 4277–4287, Oct. 2016.
- [7] Z.-Y. Xiong, Z.-H. Xu, L. Zhang, and S.-P. Xiao, "Cluster analysis for the synthesis of subarrayed monopulse antennas," *IEEE Trans. Antennas Propag.*, vol. 62, no. 4, pp. 1738–1749, Apr. 2014.
- [8] P. Rocca, G. Oliveri, R. J. Mailloux, and A. Massa, "Unconventional phased array architectures and design methodologies—A review," *Proc. IEEE*, vol. 104, no. 3, pp. 544–560, Mar. 2016.
- [9] P. Rocca, R. J. Mailloux, and G. Tosio, "GA-based optimization of irregular subarray layouts for wideband phased arrays design," *IEEE Antennas Wireless Propag. Lett.*, vol. 14, pp. 131–134, 2015.
- [10] H. Hang, L. Lili, H. Yi, and W. Qun, "Subarray weighting method for sidelobe suppression of difference pattern based on genetic algorithm," in *Proc. IEEE Antennas Propag. Soc. Int. Symp.*, San Diego, CA, USA, Jul. 2008, pp. 1–4.
- [11] S. Caorsi, A. Massa, M. Pastorino, and A. Randazzo, "Optimization of the difference patterns for monopulse antennas by a hybrid real/integer-coded differential evolution method," *IEEE Trans. Antennas Propag.*, vol. 53, no. 1, pp. 372–376, Jan. 2005.
- [12] F. Yang, Y. Ma, W. Long, L. Sun, Y. Chen, S.-W. Qu, and S. Yang, "Synthesis of irregular phased arrays subject to constraint on directivity via convex optimization," *IEEE Trans. Antennas Propag.*, vol. 69, no. 7, pp. 4235–4240, Jul. 2021.
- [13] Z. D. Qi, Y. C. Bai, Q. Wang, X. G. Zhang, and H. Chen, "Synthesis of pattern reconfigurable sparse arrays via sequential convex optimizations for monopulse radar applications," *J. Electromagn. Waves Appl.*, vol. 34, no. 2, pp. 183–200, Jan. 2020.
- [14] X. Chen, Y. Sun, F. Xu, and X. Yang, "Sub-array partition method based on particle swarm optimisation for large aperture phased array radar," *J. Eng.*, vol. 2019, no. 19, pp. 6318–6321, Oct. 2019.
- [15] W. Dong, Z.-H. Xu, X.-H. Liu, L.-S.-B. Wang, and S.-P. Xiao, "Modular subarrayed phased-array design by means of iterative convex relaxation optimization," *IEEE Antennas Wireless Propag. Lett.*, vol. 18, no. 3, pp. 447–451, Mar. 2019.
- [16] W. Dong, Z.-H. Xu, X.-H. Liu, L.-S.-B. Wang, and S.-P. Xiao, "Irregular subarray tiling via heuristic iterative convex relaxation programming," *IEEE Trans. Antennas Propag.*, vol. 68, no. 4, pp. 2842–2852, Apr. 2020.
- [17] C. Jiyuan, Z.-H. Xu, and X. Shunping, "Irregular subarray design strategy based on weighted L1 norm iterative convex optimization," *IEEE Antennas Wireless Propag. Lett.*, vol. 21, no. 2, pp. 376–380, Feb. 2022.

- [18] X. Zhao, Q. Yang, and Y. Zhang, "Synthesis of minimally subarrayed linear arrays via compressed sensing method," *IEEE Antennas Wireless Propag. Lett.*, vol. 18, no. 3, pp. 487–491, Mar. 2019.
- [19] Z. Lin, H. Hu, S. Lei, B. Jiang, B. Chen, and Q. Xie, "Synthesis of linear sub-array based on hybrid method," in *Proc. IEEE 4th Int. Conf. Electron. Inf. Commun. Technol. (ICEICT)*, Xian, China, Aug. 2021, pp. 787–789.
- [20] P. Rocca, L. Poli, N. Anselmi, and A. Massa, "Nested optimization for the synthesis of asymmetric shaped beam patterns in subarrayed linear antenna arrays," *IEEE Trans. Antennas Propag.*, vol. 70, no. 5, pp. 3385–3397, May 2022.
- [21] D. Wang, "The subarray division for the phase array radar," *Proc. SPIE*, vol. 10643, pp. 227–236, May 2018.
- [22] K. Yang, Y. Wang, and H. Tang, "A subarray design method for low sidelobe levels," *Prog. Electromagn. Res. Lett.*, vol. 89, pp. 45–51, 2020.
- [23] Q. Zhao, P. Gu, D. Ding, and R. Chen, "Pattern synthesis of planar phased arrays via subarray division with user freedom," in *Proc. Cross Strait Radio Sci. Wireless Technol. Conf. (CSRSWTC)*, Fuzhou, China, Dec. 2020, pp. 1–3.
- [24] Y. Gong, S. Xiao, Y. Zheng, and B. Wang, "An effective hybrid synthesis strategy of multibeam subarray," *IEEE Trans. Antennas Propag.*, vol. 70, no. 4, pp. 2623–2632, Apr. 2022.
- [25] Z. Lin, H. Hu, B. Chen, S. Lei, J. Tian, and Y. Gao, "Shaped-beam pattern synthesis with sidelobe level minimization via nonuniformly-spaced subarray," *IEEE Trans. Antennas Propag.*, vol. 70, no. 5, pp. 3421–3436, May 2022.
- [26] Z.-Y. Xiong, Z.-H. Xu, S.-W. Chen, and S.-P. Xiao, "Subarray partition in array antenna based on the algorithm X," *IEEE Antennas Wireless Propag. Lett.*, vol. 12, pp. 906–909, 2013.
- [27] M. Sivasankar and R. M. Hegde, "Subarray design for multibeam radars with clustering methods," in *Proc. 21st Int. Radar Symp. (IRS)*, Warsaw, Poland, Oct. 2020, pp. 286–291.
- [28] C.-Y. Cui, Y.-C. Jiao, L. Zhang, L. Lu, and H. Zhang, "Synthesis of subarrayed monopulse arrays with contiguous elements using a DE algorithm," *IEEE Trans. Antennas Propag.*, vol. 65, no. 8, pp. 4340–4345, Aug. 2017.
- [29] E. Juárez, M. A. Panduro, A. Reyna, D. H. Covarrubias, A. Mendez, and E. Murillo, "Design of concentric ring antenna arrays based on subarrays to simplify the feeding system," *Symmetry*, vol. 12, no. 6, p. 970, Jun. 2020.



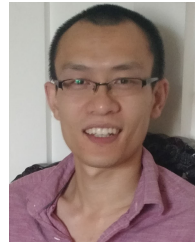
**KE WANG** received the B.S. degree in communication engineering from Jiangxi Normal University, Nanchang, China, in 2021. She is currently pursuing the M.S. degree with the School of Electronic Information, Nanjing University of Aeronautics and Astronautics (NUAA), Nanjing, China.

Her current research interest includes array signal processing.



**HAILIN LI** received the Ph.D. degree in signal and information processing from the Nanjing University of Aeronautics and Astronautics (NUAA), Nanjing, China, in 2013.

He is currently an Associate Professor with the College of Electronic and Information Engineering, NUAA. His research interests include digital signal processors, conformal array, and array signal processing



**YUAN DING** (Member, IEEE) received the bachelor's degree in electronic engineering from Beihang University (BUAA), Beijing, China, in 2004, the master's degree in electronic engineering from Tsinghua University, Beijing, in 2007, and the Ph.D. degree in electronic engineering from Queen's University Belfast, Belfast, U.K., in 2014.

He was a Radio Frequency (RF) Engineer with the Motorola Research and Development Centre, Beijing, from 2007 to 2009, before joining Freescale Semiconductor Inc., Beijing, as an RF Field Application Engineer, responsible for high power base-station amplifier design, from 2009 to 2011. He is currently an Assistant Professor with the Institute of Sensors, Signals and Systems (ISSS), Heriot-Watt University, Edinburgh, U.K. His research interests include the IoT-related physical-layer designs, antenna array, physical layer security, and 5G related areas.

Dr. Ding was a recipient of the IET Best Student Paper Award from LAPC 2013 and the Young Scientists Awards in General Assembly and Scientific Symposium (GASS) from the 2014 XXXIst URSI.



**JING TAN** received the M.S. degree in signal and information processing from the Nanjing University of Aeronautics and Astronautics (NUAA), Nanjing, China, in 2006, where she is currently pursuing the Ph.D. degree.

She is an Associate Professor with the Department of Information Engineering, Nanhang Jincheng College, China. Her research interest includes the study of antenna array signal processing.



**XIAO DONG** received the bachelor's degree from the North China University of Water Resources and Electric Power, Zhengzhou, China, in 2021. She is currently pursuing the M.S. degree with the Nanjing University of Aeronautics and Astronautics. Her current research interests include array signal processing and array theory and technology.

• • •